ELSEVIER

Thermochimica Acta 392–393 (2002) 271–287

thermochimica acta

www.elsevier.com/locate/tca

Investigations on flammability models and zones for *o*-xylene under various initial pressures, temperatures and oxygen concentrations

Chi-Min Shu*, Po-Jiun Wen, Ron-Hsin Chang

Process Safety and Disaster Prevention Laboratory, Department of Environmental and Safety Engineering, National Yunlin University of Science and Technology, 123 University Road, Section 3, Touliu, Yunlin 640, Taiwan, ROC

Received 29 December 2000; accepted 12 May 2001

Abstract

The main purpose of this study is to investigate various initial temperatures (100–230 °C) and pressures (760–2,280 mmHg) for fire and explosion characteristics of *o*-xylene (OX)/air mixtures, which are commercially used in the production of phthalic anhydride (PA), so that empirical flammability models can be established and used in calculations for flammability zones.

According to the results of the experiment, while the experimental condition of OX is controlled by the same oxygen concentration, if the initial temperature is increased, the upper explosion limit (UEL), flammability zones of OX are correspondingly increased, but the maximum explosion pressure (P_{max}) gas or vapour explosion constant (K_g) of OX is decreased. In addition, if the initial pressure is increased, the explosion characteristic parameters are all increased.

However, while OX is controlled by the same oxygen concentration, if the initial temperature is increased, the lower explosion limit (LEL) of OX is decreased. Nevertheless, if the initial pressure is increased, the LEL has various changes under various temperatures. In general, the LEL of OX has little change at higher temperature.

From the experimental results, the minimum oxygen concentration (MOC) does not significantly vary while the initial temperature is increased, whereas it will be decreased by enhancing initial pressure. Therefore, the MOC of OX is determined by initial pressure instead of initial temperature.

It is crucially important that if the initial temperature is lower than the normal boiling point of OX (144 °C), then the UEL, P_{max} and K_g of OX are higher under 100 °C than 150 °C and even higher temperatures. Consequently, the liquid–vapour co-existing phase will demonstrate higher degree of hazard. Therefore, it is important that the loading of the volume concentration of OX should not fall into the flammability zone.

Keywords: *o*-Xylene; Flammability models; Flammability zones; Explosion characteristic parameters; Liquid–vapour co-existing phase

1. Introduction

In recent years, more and more process accidents have occurred in Taiwan, especially fires and explosions—75.6% of all industrial incidents. Therefore, proactive prevention of fire and explosion hazards is the most crucial issue in process safety island-wide.

Prevention of explosion accidents in the process industries has normally been based upon the recognition of material hazards. It is important that these industries provide effective methods to avoid any

* Corresponding author.
Tel.: +886-5-534-2601x4416/4401/4402; fax: +886-5-531-2069.
E-mail address: shucm@pine.yuntech.edu.tw (C.-M. Shu).

0040-6031/02/$ – see front matter
PII: S0040-6031(02)00110-7

unexpected fire and explosion hazards, at least to control explosion ranges and damage, not to mention their ecological impact. In addition, the chemical plant could match up prevention facilities and mitigate explosion hazards to reach the lowest and acceptable level [13].

Practically speaking, combustible gases are frequently used in chemical processes. In order to evaluate the explosion hazards and to ensure safe and as well as optimal operation of these processes, it is imperative to understand the combustion characteristics under the operating or abnormal conditions, especially various temperatures and pressures that have played a key role in terms of degree of hazards in this area [3,12].

In view of the fact that the normal boiling point of *o*-xylene (OX) is 144 °C, if the experimental temperature of OX loading for the volume concentration of feed mixture is higher than the normal boiling point of OX, the OX/air mixture is hypothesised to be an ideal gas.

So far, no numerical model can predict the flammability limits in all phthalic anhydride (PA) process plants that is considered to be the prevailing and reliable method. Evidently, at ambient temperature and atmospheric pressure, these flammable limits have been well established. However, under various oxygen concentrations, along with elevated initial temperatures and pressures, they may have different explosion characteristic parameters. In this investigation, the flammability models and flammability zones of OX under various initial temperatures and pressures as well as oxygen concentrations are established and elucidated. Eventually, the explosion characteristic parameters could be fully exploited and provided to prevent PA plants from any unexpected fires and explosions.

2. Experimental apparatus and procedure

The experimental 20-L-Apparatus (or 20 litre Spherical Explosion Vessel) was obtained from Adolf Kühner AG. The test chamber is a stainless steel hollow sphere with a general acceptance of the personal computer (PC) shown in Fig. 1, as a tool making it feasible to interface the PC with the 20-L-Apparatus. Essentially, the vessel is designed to withstand explosion pressure up to 39 bara. The ignition source is located in the centre of the sphere. On the measuring flange two "Kistler" piezoelectric pressure sensors are installed. The second flange can be used for additional measuring elements or for the installation of a sight glass. A pyrotechnic igniter with a total of 10 kJ was used as ignition source for the gas/vapour system. Normally, the 20-L-Apparatus and the gas control unit KSEP 310 are set up in a ventilated laboratory hood. The other units are installed outside of the hood [22,23].

For cleaning, the sphere can be opened on top by turning the bayonet ring. The diameter of the "hand hole" is 94 mm. A larger opening of 140 mm can be obtained by unscrewing the top flange. A safety switch controls the correct closing position of the bayonet ring [17].

The desired operating conditions can be reached by a test procedure that keeps the operating temperature from between 100 and 230 °C by means of silicon oil heating and removes heat while an explosion is taking place.

In the past, the international standards have described the 1 m^3 vessel as the test apparatus. In recent years, increasing use has been made of the more convenient and less expensive 20-L-Apparatus as the standard equipment. Investigation of the explosion behaviour of combustible materials (combustible dusts, flammable gases, or solvent vapours) must be performed in accordance with internationally recognised test procedures [1,2].

The purpose of our flammability testing was to define the flammability concentration limits for OX vapour at given temperature and pressure, along with specific oxygen concentration. For these studies quiescent gases at initial temperatures from 100, 150, 200, 230 °C and three kinds of pressures of 760, 1,520,

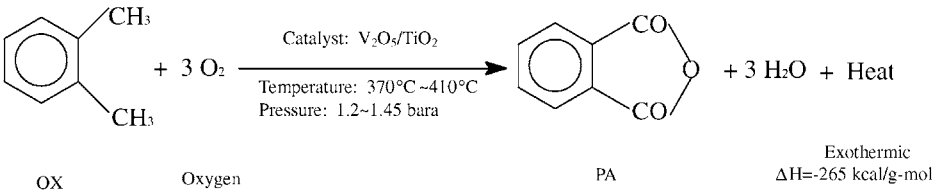

Fig. 1. A typical PA process with its reaction chemistry.

2,280 mmHg were established. Along with the determination of the flammability envelope, peak pressures and maximum rates of pressure rises will be measured throughout many of the flammability zones. These fire and explosion characteristics of OX will be used to establish flammability models, to continuously calculate for flammability zones and to evaluate degree of the hazards while enhancing the oxygen concentration in the mixtures. In addition, by predictive flammability models, the hazards in the OX on flammability zones can be determined.

The use of the OX flammability zones could avoid fire and explosion hazards under different process conditions. Meanwhile, it could also provide an important standard for protecting the PA plant from fire and explosion hazards.

3. Oxidation process of PA

Commercially, PA is an important chemical whose major applications are: (1) process plasticity dosage (dioctyl phthalate (DOP)); (2) paint; (3) unsaturated polyester resins (UPR); (4) intermediate for dyes; (5) an ingredient for medicine and spices and so on. To manufacture PA, there are two kinds of raw materials: OX and naphthalene, but the former has prevailed. [9,10,24] PA can be produced from OX by catalytic oxidation with air by the following reaction, as shown in Fig. 2 [6,14,19].The crude PA from the condensers is above 99 mol% purity, with phthalic acid and *p*-xylene (PX) being the major impurities. The purity of OX is more than 99 wt.%, with other residues such as PX, cumene, *m*-xylene (MX) and styrene. The major residue is PX and the concentration of cumene should be controlled under 0.3 wt.%.

4. Literature review

4.1. Flammability limit dependence on temperature

In general, the flammability range increases with initial temperature. The following empirically derived equations are available for vapours [11,26].

$$\mathrm{UEL}_T = \mathrm{UEL}_{25}\left[1 - \frac{0.75(T_0 - 25)}{\Delta H_c}\right] \quad (1)$$

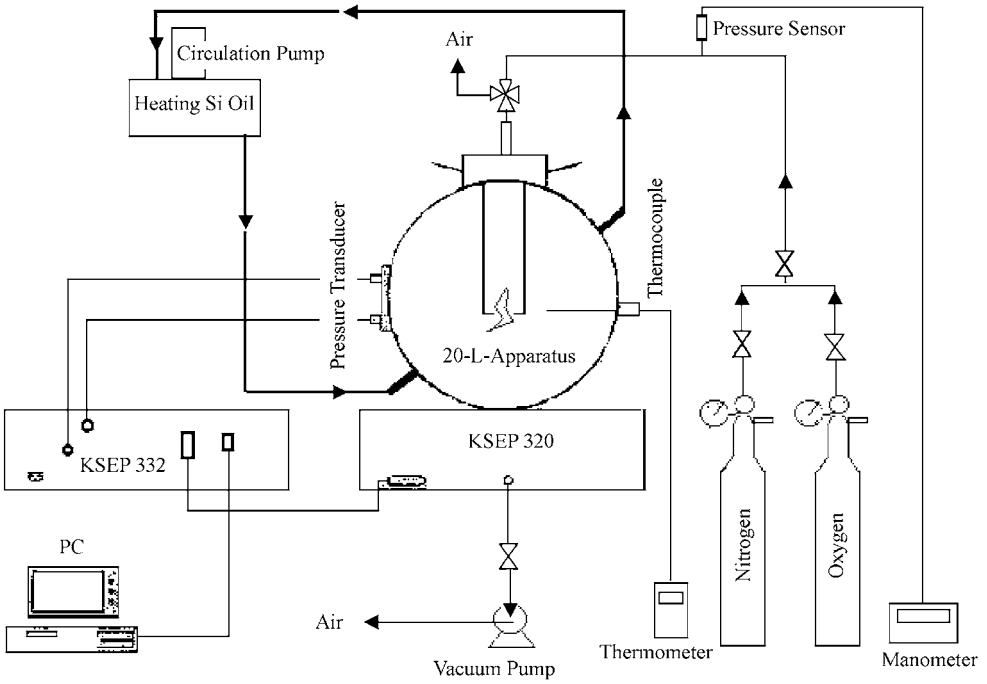

Fig. 2. A schematic diagram of the 20-L-Apparatus with control system.

where ΔH_c is the net heat of combustion, (kcal/mole), T_0 the temperature (°C). Temperature dependence of the upper explosion limit (UEL) at various initial pressures can be shown in Eq. (2) [25,27].

$$\mathrm{UEL}(T_1) = \mathrm{UEL}(T_0)\left[1 + c\left(\frac{T_1 - T_0}{100}\right)\right] \quad (2)$$

According to the four different OX conditions, UELs were obtained based upon the different initial temperatures (100, 150, 200, 230 °C). The coefficient c can be fed to Eq. (2). By Eq. (2), the PA process plant could readily forecast OX UELs under higher temperatures. Therefore, by three different initial pressures under these four temperatures that are established to formulate flammability zones from the OX UELs, the area can be analysed and its variation evaluated.

4.2. Flammability limit dependence on pressure

As far as pressure is concerned, the initial pressure has no remarkable effect on the lower explosion limit (LEL) except at very low pressure (<50 mmHg absolute), where flames do not propagate. However, the UEL increases significantly as the initial pressure is increased, broadening the flammability range. Eq. (3) is an empirical expression for the UEL for vapours as a function of pressure [7,24].

$$\mathrm{UEL}_P = \mathrm{UEL} + 20.6(\log P + 1) \quad (3)$$

where P is the pressure (MPa absolute) and UEL the upper flammability limit (vol.% of fuel at 760 mmHg).

However, the empirical expression for the UEL for vapours as a function of pressure is not available for all gases/vapours. Nevertheless, an empirical model can be created for the UEL specifically for OX through the regression of experimental data.

Vanderstraeten et al. [25] correlated their data to an equation for the pressure dependence of the UEL Eq. (4) [4,24].

$$\mathrm{UEL}(P_1) = \mathrm{UEL}(P_0)\left[1 + a\left(\frac{P_1}{P_0} - 1\right) + b\left(\frac{P_1}{P_0} - 1\right)^2\right] \quad (4)$$

Accordingly, the OX experimental data are then used by Eq. (3) to estimate the UEL at different initial pressures. If the error in UEL by using Eq. (3) is significant, then coefficients a and b can be substituted into Eq. (4). In general, the prediction of UEL by the empirical model of Eq. (4) is practically close to the real UEL of OX.

4.3. Flammability limit dependence on oxygen concentration

Coward and Jones had established empirical expressions on increasing oxygen concentration 21–100 vol.% for hydrocarbons that can be expressed as Eq. (5) [8].

$$\mathrm{UEL}_{(\mathrm{O_2\ vol.\%})} = \mathrm{UEL}_{(\mathrm{O_2\ 20.95\ vol.\%})} + p[\log(\mathrm{O_2\ vol.\%}) - q] \quad (5)$$

All the OX UELs under testing experiment can be controlled at the same pressures and temperatures. Then the different OX UELs can be obtained based upon the increasing oxygen concentration from 30 to 40 vol.%. The coefficients p and q can be fed to Eq. (5). By Eq. (5), the PA plant can predict OX UELs under higher oxygen concentration that the apparatus could not reach, because the 20-L-Apparatus is designed to withstand explosion pressure only up to 39 bara. Accordingly, the OX flammability zones can be established more completely under a wider spectrum.

4.4. Flammability diagram

According to the following combustion equation, the Z is 10.5 which can be used to form the flammability diagram. The stoichicometric line could be established by Eqs. (6) and (7). Equation (8) is the intersection of the stoichicometric line with the oxygen axis.

$$\mathrm{OX} + 10.5\,\mathrm{O_2} \rightarrow 8\mathrm{CO_2} + 5\mathrm{H_2O} + \mathrm{Heat} \quad (6)$$

$$1\,\mathrm{Fuel} + Z\mathrm{O_2} \rightarrow \mathrm{Product} \quad (7)$$

$$\left(\frac{Z}{1+Z}\right)100 \quad (8)$$

From the flammability diagram, a point called out of service fuel concentration (OSFC) is used to avoid entering the flammability zone when air is introduced to the vessel containing 100% fuel. Similarly, a point called in service oxygen concentration (ISOC) is applied to keep oxygen concentration truly below MOC while fuel is introduced into the vessel [5,18,24].

The OSFC and ISOC are calculated by Eqs. (9) and (10) [5].

$$\mathrm{OSFC_{MOC}} = \frac{\mathrm{MOC}}{Z(1 - \mathrm{MOC}/21)} \quad (9)$$

$$\mathrm{ISOC_{MOC}} = \frac{\mathrm{MOC} \times Z}{(Z - \mathrm{MOC}/100)} \quad (10)$$

5. Results and discussion

For a typical loading, the volume concentration of OX would be 1.2–1.5 vol.% of the feed mixture. In practice, process conditions for normal PA plants are controlled under 370–410°C, 760 mmHg initial temperature and 760 mmHg and initial pressure, respectively.

Based upon the test results, as the experimental conditions of OX are controlled under various initial pressures and initial temperatures, by the Ideal Gas Law, the P_{max} of OX are different under the various OX concentrations as shown in Fig. 3. It indicates in the relationship on OX concentration versus P_{max}, that (gas pressure/explosion), while the initial temperature is set at 100 °C and 760 mmHg as initial pressure and the oxygen concentration, the OX concentration is in the range of 11–40 vol.%. Then the UEL as well as LEL of OX are also determined. Here, the P_{max} are zero at two different extremities along each curve. Therefore, the explosion characteristic parameters, such as LEL and UEL, are strongly related with OX concentrations.

Fig. 4 shows the OX concentration versus $(dP/dt)_{max}$. In addition, while OX is under various initial temperatures and initial pressures, it will be compared with all explosion characteristic parameters on figures by various mixtures under experimental conditions, as shown in Figs. 4–9.

From Fig. 5 as the experimental conditions of OX are controlled at 760 mmHg, 21 vol.%, and 150–230 °C as initial pressure, oxygen concentrations and initial temperatures, respectively, the UEL of OX is increased from 5.5 to 6.25 vol.%. This demonstrates that the greater the initial temperature, the greater the reaction rate, corresponding to the larger of the explosion limits. However, from the experimental results, the UEL of OX is a little bit larger under 100 than 150 °C, but is slightly less than 200 and

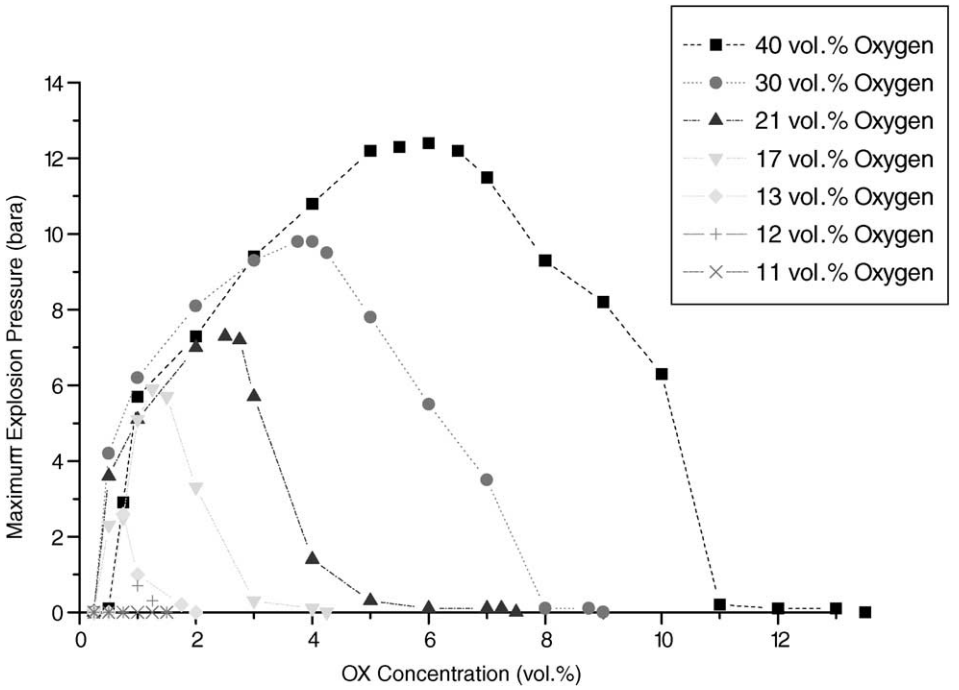

Fig. 3. P_{max} vs. OX concentration at 100 °C/760 mmHg.

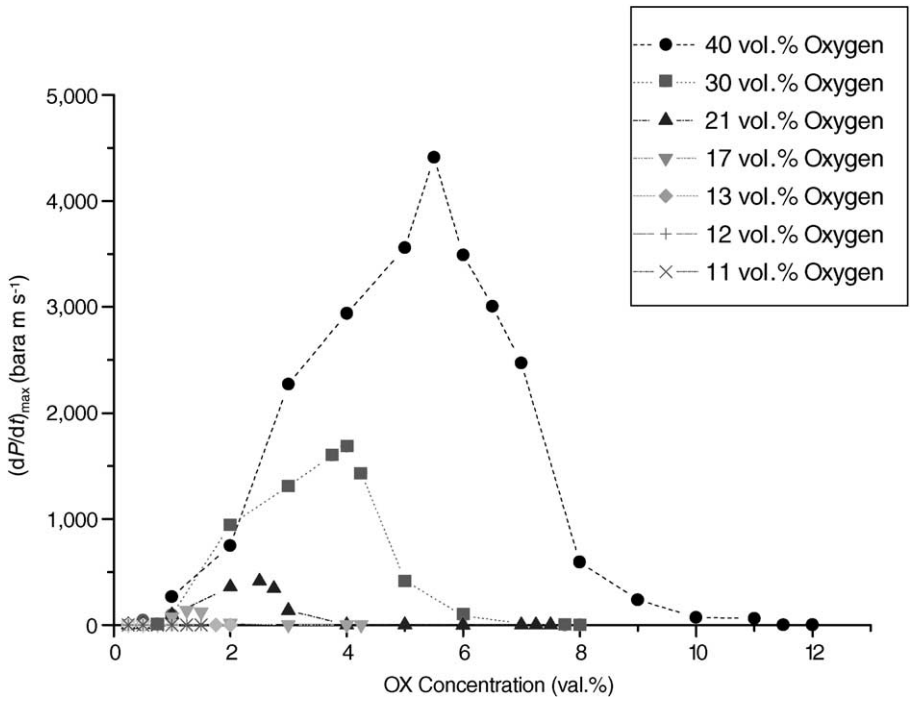

Fig. 4. $(dP/dt)_{max}$ vs. OX concentration at 100 °C/760 mmHg.

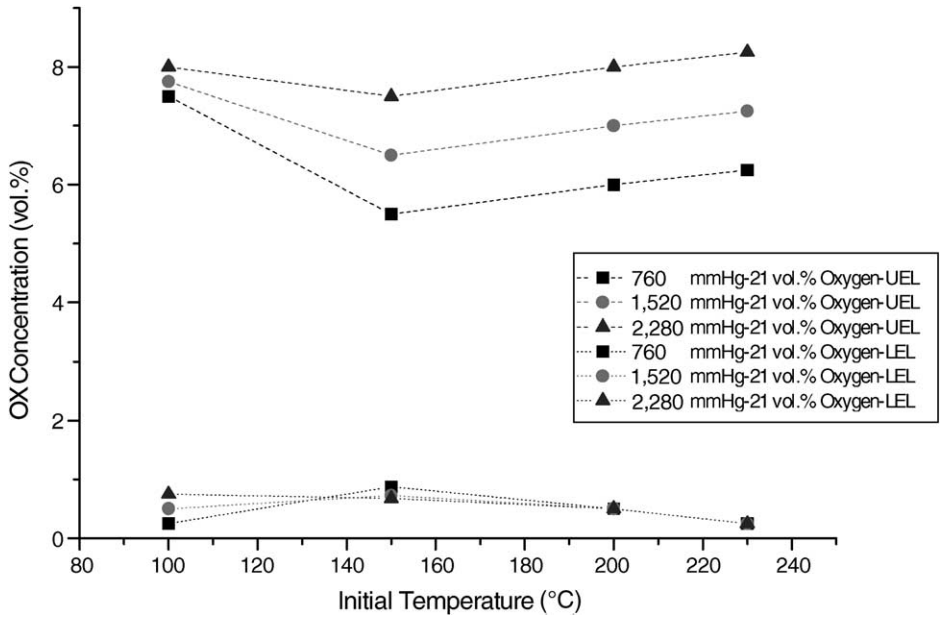

Fig. 5. LEL and UEL concentration vs. initial temperature with OX at initial pressures ranging from 760 to 2,280 mmHg at 21 vol.% oxygen.

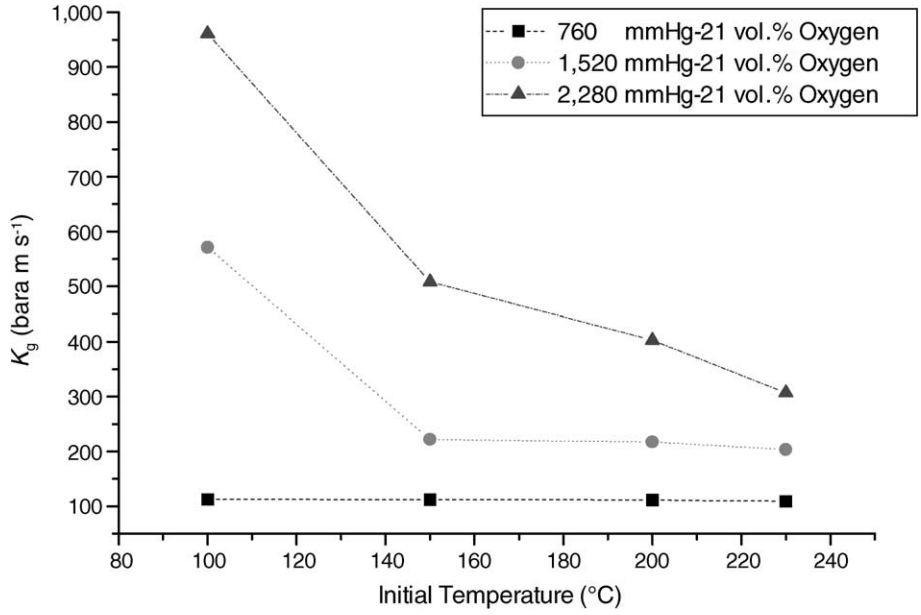

Fig. 6. P_{max} vs. initial temperature with OX at initial pressures ranging from 760 to 2,280 mmHg at 21 vol.% oxygen.

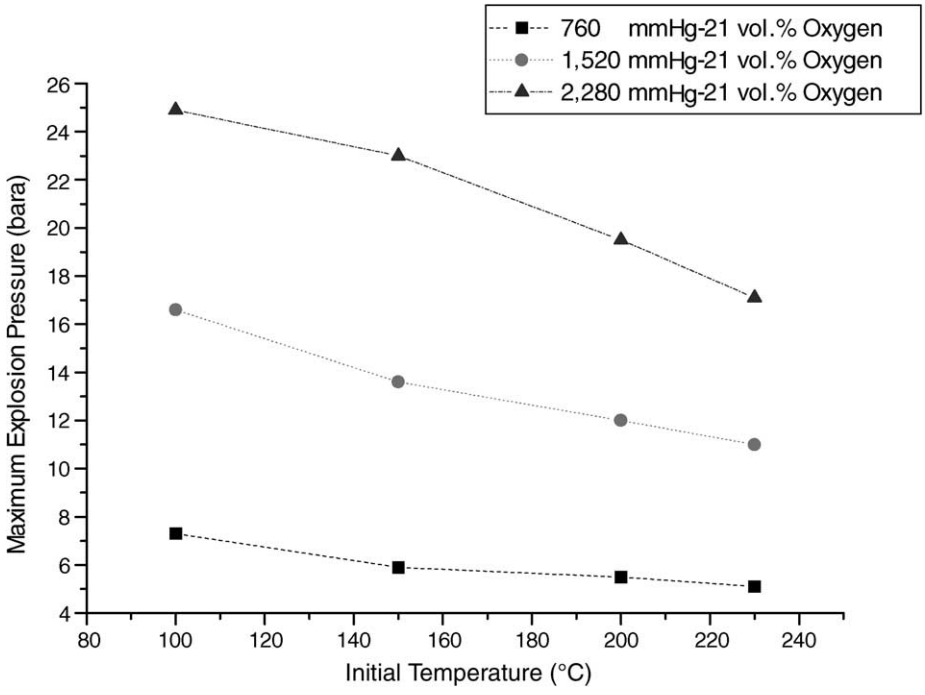

Fig. 7. K_g vs. initial temperature with OX at initial pressures ranging from 760 to 2,280 mmHg at 21 vol.% oxygen.

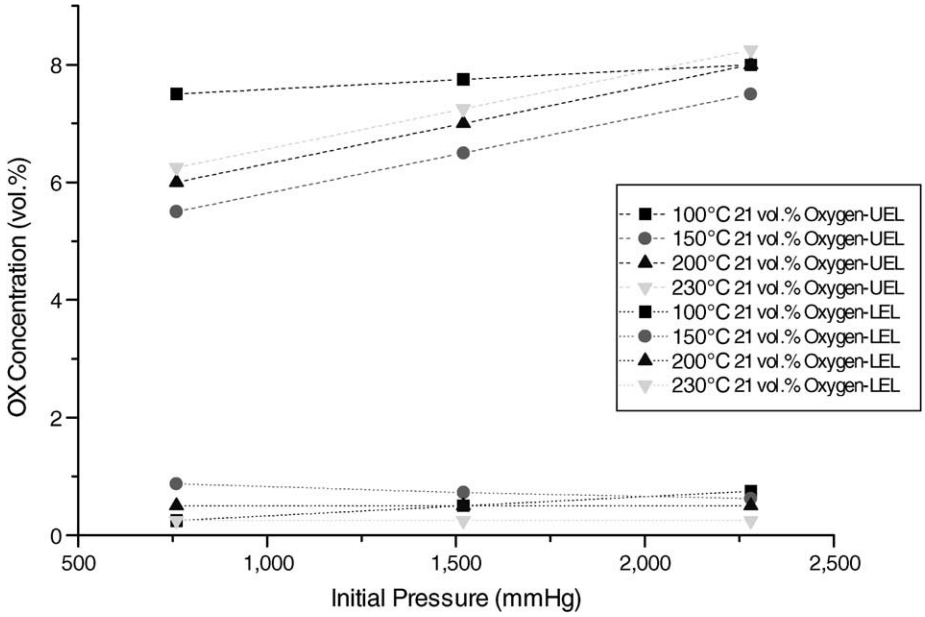

Fig. 8. LEL and UEL concentration vs. initial pressure with OX at initial temperatures ranging from 100 to 230 °C at 21 vol.% oxygen.

230 °C. At 100 °C, which is lower than 144 °C of the OX normal boiling point, the liquid–vapour co-existing phenomenon is produced. Meanwhile, Fig. 5. also shows that the LEL variation is negligible in that all the LELs of OX are relatively small. Therefore, according to the experimental results, these LELs are not as significant as UELs. As shown in Fig. 6, while the experimental conditions of OX are controlled at

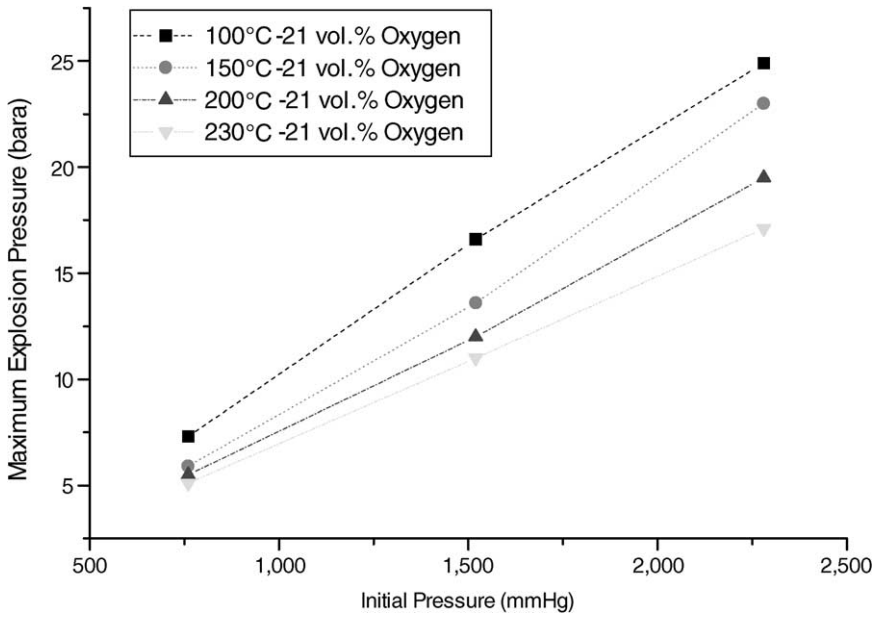

Fig. 9. P_{max} vs. initial pressure with OX at initial temperatures ranging from 100 to 230 °C at 21 vol.% oxygen.

760 mmHg as the initial pressure, along with 21 vol.% of oxygen concentration, P_{max} of OX is decreased from 5.9 to 5.1 bara, corresponding to 150–230 °C of initial temperature.

As the initial temperature is increased, the P_{max} of OX are conversely decreased. Apparently, the results also illustrate that the OX vapour is filled with air in the vessel under higher temperature, so the amount of OX liquid residue at the bottom of the vessel is relatively less than the lower one (*T*). Hence, as the initial temperature is 100 °C, it may have such results. Strictly speaking, this is because the OX normal boiling point is 144 °C, producing higher P_{max} with liquid–vapour co-existing system. As shown in Fig. 7, as the experimental conditions of OX are controlled at 760 mmHg as initial pressure, along with 21 vol.% of oxygen concentration, K_g of OX is decreased from 112.19 to 108.9 m bara s^{-1}, corresponding to 150–230 °C of initial temperature.

Accordingly, while the temperature is increased, the K_g of OX is decreased. Especially, the slope of the curve is steeper from 100 to 150 °C than from 150 to 230 °C. From the open literature, the K_g of OX can be equivalent to St-classes that can be, in turn, used to decide its hazard classes. Therefore, while the experimental conditions of OX are controlled at the same pressure, the degree of hazard of OX occurring under 100 °C is greater than other higher temperatures. In other words, under operating ranges, if the initial temperature is higher, the hazard of OX will be lower, because the liquid density of OX is much greater than the vapour one.

As shown in Fig. 8, as the experimental conditions of OX are controlled at 230 °C as initial temperature, along with 21 vol.% of oxygen concentration, UEL of OX is increased from 6.25 to 8.25 vol.%, corresponding to 760–2,280 mmHg of initial pressure. Under other temperature conditions, the experimental results are similar. Possible reasons could be that while the initial pressure is increased, the molecular concentration, the reaction rate, and the heat of combustion of OX are proportionally increased with different extents.

However, according to the LEL of OX, the results indicate that there is no significant change. In addition, the LEL variation is kept within the range of 0.25 vol.%. As shown in Fig. 9, while the experimental conditions of OX are controlled at 230 °C as initial temperature, along with 21 vol.% of oxygen concentration, P_{max} of OX is monotonically increased from 5.1 to 17.1 bara, corresponding to 760–2,280 mmHg of initial pressure. By enhancing the initial pressure from 760 to 2,280 mmHg, it will correspondingly increase the P_{max}, enhancing the increase of OX concentration.

As shown in Fig. 10, while the experimental conditions of OX are controlled at 230 °C as initial temperature, along with 21 vol.% of oxygen concentration, K_g of OX is increased from 108.9 to 306.8 m bara s^{-1}, corresponding to 760–2,280 mmHg of initial pressure. The K_g is computed and corresponds to explosion classes (St) from literature. Here the experimental result of OX as shown in Fig. 10, the St = 1 switches to St = 3 while the K_g of OX is increased from 108.9 to 306.8 m bara s^{-1} [15].

However, the St = 3 of OX, during initial pressure of 1,520 mmHg and initial temperature of 100 °C, shows that the degree of hazard is even higher than 2,280 mmHg as initial pressure at temperature higher than 100 °C of initial temperature. This is because the St = 2 of OX, during initial pressure of 2,280 mmHg at a temperature higher than 100 °C as initial temperature.

As shown in Fig. 11, while the experimental conditions of OX are controlled at 150 °C as initial temperature and 760 mmHg as initial pressure, and increased oxygen concentration from 12 to 40 vol.%, the UEL of OX is changed from 0 to 13.25 vol.%, so the MOC is decided to be 12 vol.%. However, if oxygen concentration is linearly increased, then the UEL is increased with the same ratio. Likewise, this result can be applied to other initial temperatures and pressures.

As shown in Fig. 12, if the experimental conditions of OX are controlled at 150 °C as initial temperature and 760 mmHg as initial pressure, then increasing oxygen concentration from 12 to 40 vol.% will have the P_{max} of OX enhanced from 0 to 10.1 bara.

Under lower oxygen concentration, the variation of P_{max} of OX is slightly small but is quite remarkable under higher oxygen concentration. Therefore, while increasing oxygen concentration, the P_{max} of OX is divergently increased. Similarly, this result can be applied to other initial temperatures and pressures.

As shown in Fig. 13, while the experimental conditions of OX are controlled at 150 °C as initial temperature and 760 mmHg as initial pressure, along with increased oxygen concentration from 21 to 40 vol.%, the K_g of OX is increased from 0 to 788.8 m bara s^{-1}. The K_g can be calculated to specifically identify the

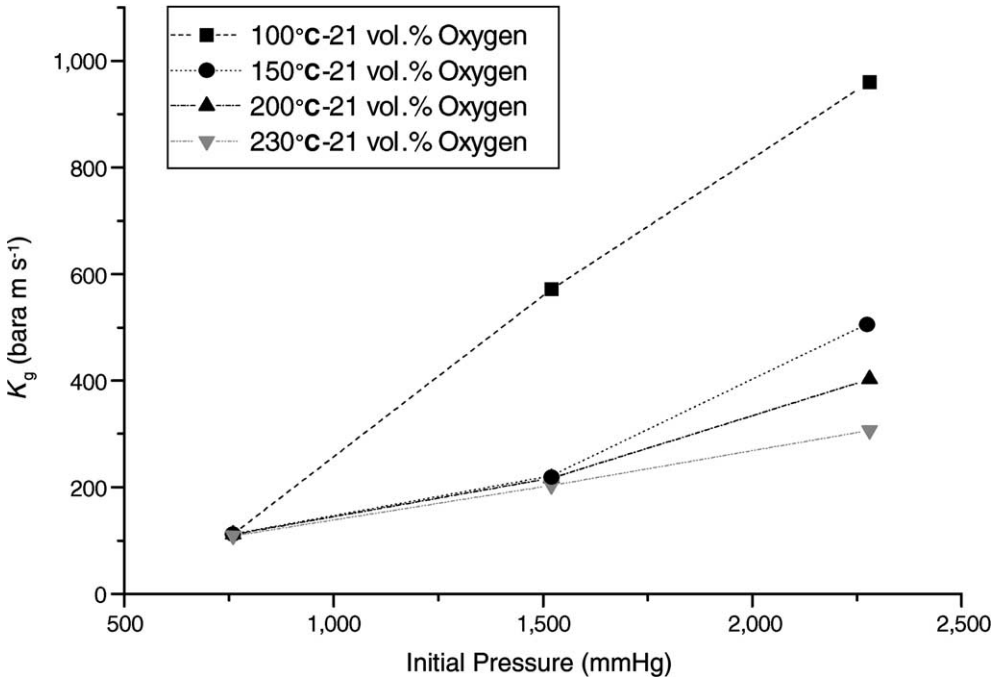

Fig. 10. K_g vs. initial pressure with OX at initial temperatures ranging from 100 to 230 °C at 21 vol.% oxygen.

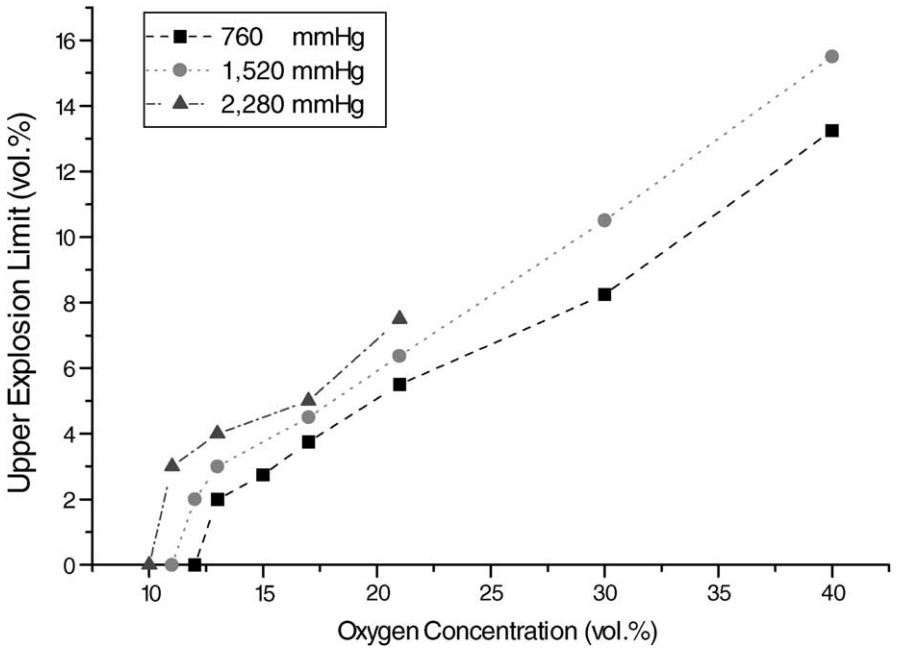

Fig. 11. UEL vs. oxygen concentration with OX at 150 °C and three different initial pressures.

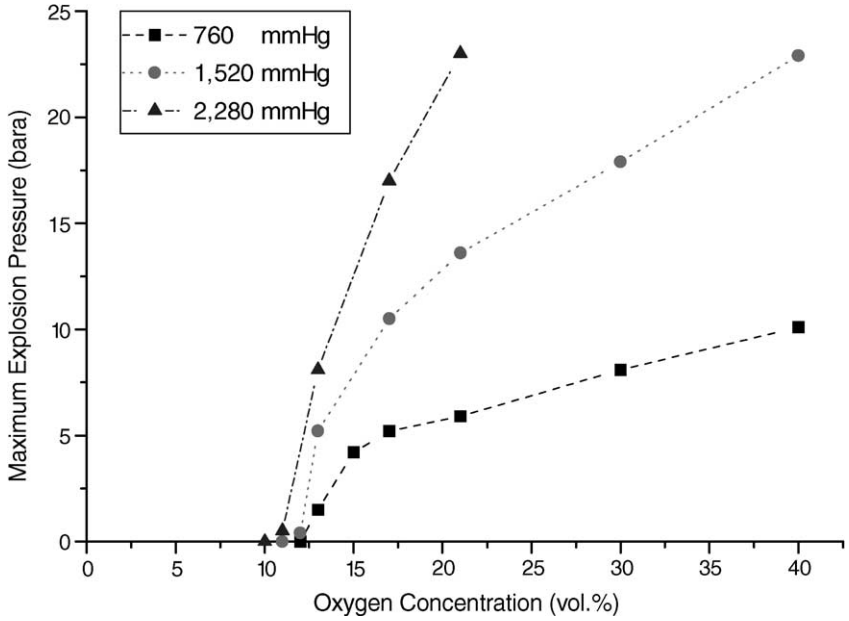

Fig. 12. P_{max} vs. oxygen concentration with OX at 150 °C and three different initial pressures.

explosion classes (St) from literature. Fig. 13 demonstrates the experimental result of OX, explosion characteristic, switching from St = 0 to St = 3 as the K_g of OX are increased from 0 to 788.8 m bara s^{-1}.

Therefore, while oxygen concentration is increased, the K_g of OX is increased and the degree of hazard is increased, also. Practically speaking, the result can also be applied to other various initial temperatures

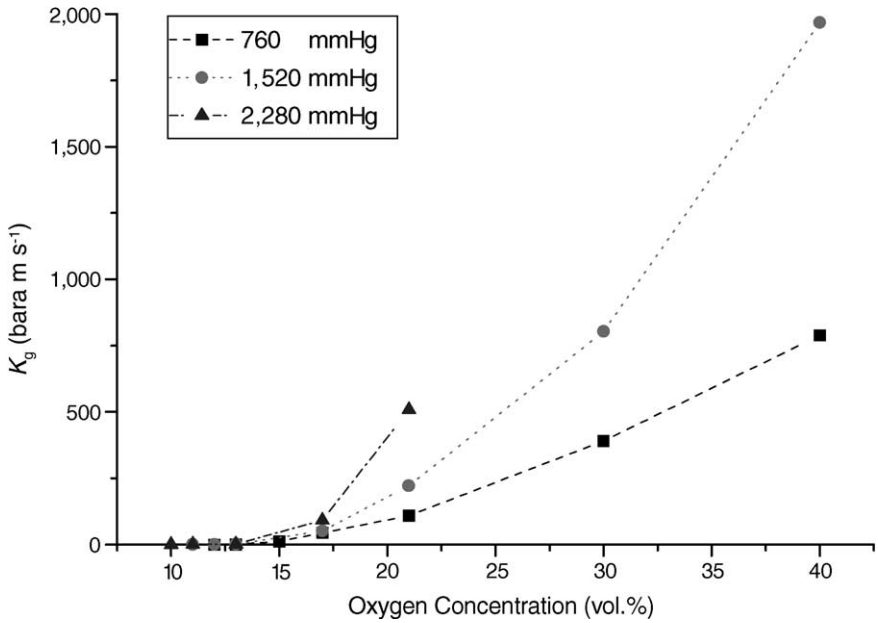

Fig. 13. K_g vs. oxygen concentration with OX at 150 °C and three different initial pressures.

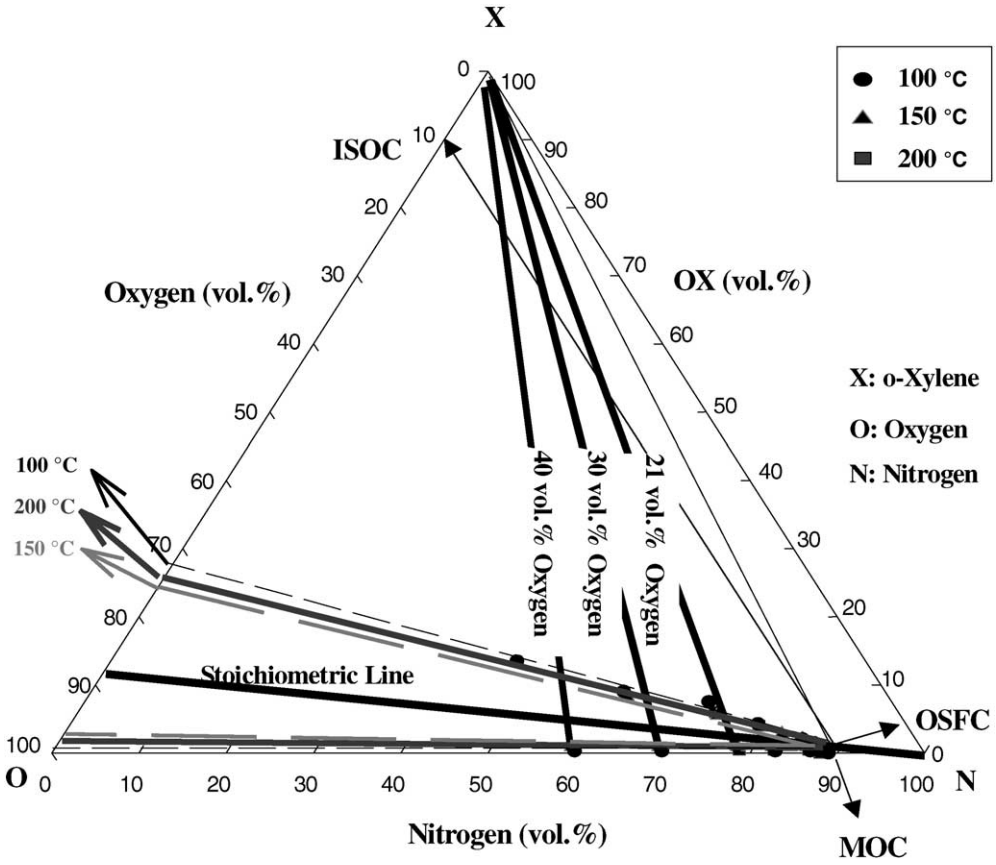

Fig. 14. Overall triangular flammability diagram contrasting the change in flammability zone with OX at 760 mmHg and three different initial temperatures.

and pressures. Based upon the above combustion reaction Eq. (6), the value of Z is 10.5, as from the corresponding Eq. (7). Therefore, the stoichiometric line of OX is determined to be 91.3 vol.%.

The MOC is 10 vol.% under experimental conditions of 100 °C as initial temperature and 2280 mmHg as initial pressure. In essence, this is most conservative method for avoiding any hazards. Meanwhile, the OSFC and ISOC for the triangular flammability diagram of OX were determined to be 1.8 and 10.1 vol.%, respectively. Most of the explosion characteristic parameters are identified through the triangular flammability diagram as shown in Fig. 14, along with calculated flammability zones.

Fig. 14 shows that while the experimental conditions of OX are controlled at 760 mmHg as initial pressure, the flammability zone is changed from 25 to 28 vol.% as initial temperature switches from 150 to 200 °C. Therefore, the flammability zones are increased from having the initial temperatures raised.

However, the flammability zone is 32% under 100 °C, which is greater than 150 and 200 °C. The result is mainly due to the liquid–vapour co-existing phenomenon that can result in larger flammability zones. The flammability zone, which while the initial temperature of OX for experimental conditions is higher than 200 °C, will be larger than 100 °C. However, it is possible that, at a higher temperature, such as 300 °C, the flammability zone may have larger area than one at 100 °C.

With the results from increasing initial temperatures and initial pressures of OX, all the explosion characteristic parameters, such as UEL, LEL and MOC, could be identified in triangular flammability diagram

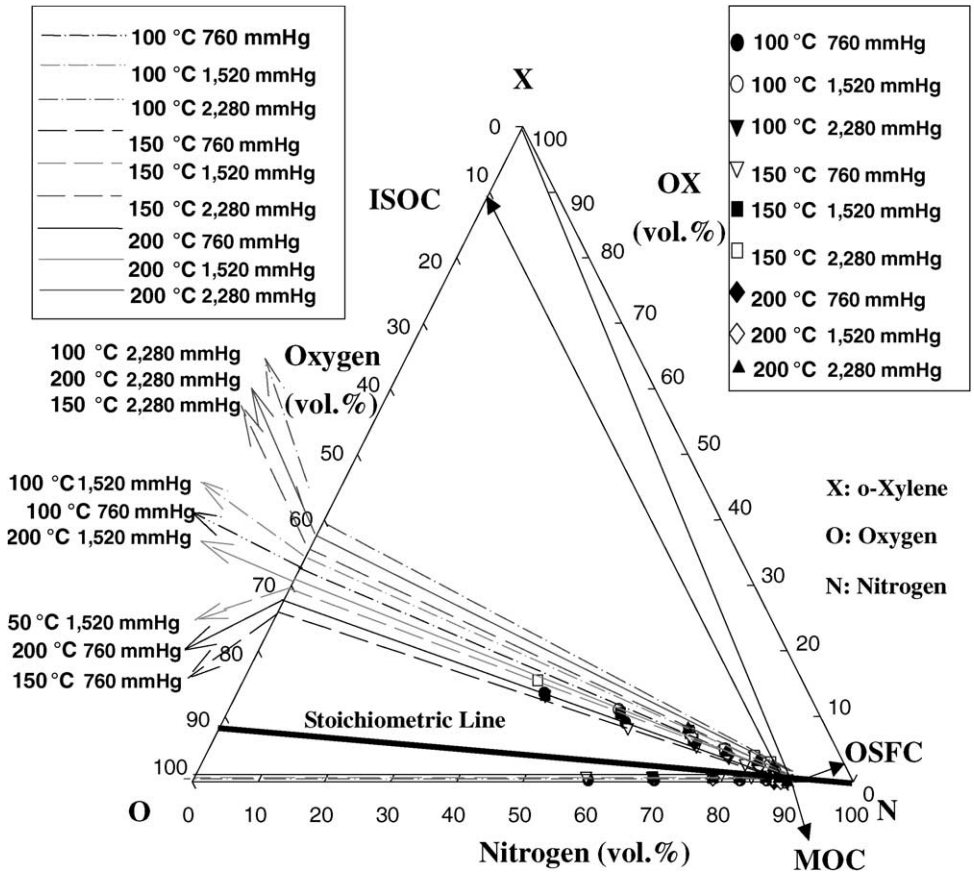

Fig. 15. Overall triangular flammability diagram contrasting the change in flammability zone with OX at three different initial temperatures and three different initial pressures.

as shown in Fig. 15. As shown in Fig. 15, under various initial temperatures of OX, the flammability zone at 2,280 mmHg as initial pressure of OX is larger than 1,520 and 760 mmHg. Therefore, while initial pressure is increased, the flammability zone of OX will be proportionally increased.

Whereas, while initial temperature is increased, the flammability zone of OX will be increased, too. On the other hand, the flammability zone of OX under 100 as initial temperature and 760 mmHg as initial pressure, is larger than 150 and 200 °C with 1,520 mmHg, respectively. The areas of the flammability zones of OX are calculated and shown in Tables 1 and 2.

While initial temperature is 100 °C and initial pressure is increased from 760 to 2,280 mmHg of OX, the areas of flammability zones are increased from 32 to 38%. With initial pressure of 760 mmHg, as initial temperature of OX is increased, the areas of flammability zones of OX are increased, also.

However, the areas of flammability zones of OX are 32% under 100 °C for initial temperature, that is larger than 25% for 150 °C and 28% for 200 °C as initial temperature, respectively.

Table 1
Vapour pressure of OX with respect to its corresponding temperature

Temperature (°C)	Vapour pressure (mmHg)
100	197 (3.8 psia)
150	879 (17 psia)
200	2,844 (55 psia)
230	4,757 (92 psia)

Table 2
Flammability zones for OX under various temperatures and pressures

Temperature (°C)	Pressure (mmHg)	Flammability zones ratio (%)
100	760	32
100	1,520	34
100	2,280	38
150	760	25
150	1,520	30
150	2,280	35
200	760	28
200	1,520	31
200	2,280	37

The literature review provides many explosion empirical expressions for hydrocarbons. However, the empirical model for the UEL of vapours as a function of temperature is not available for all gases/vapours. Nevertheless, an empirical model can be created for the UEL specifically for OX by the regression of experimental data. To avoid having the OX concentration fall into the flammability zone under increasing initial temperatures and initial pressures, the experimental data can be manipulated to find a close empirical model of the UEL for OX.

Vanderstraeten, et al. correlated their data to an equation for the temperature dependence of the UEL, as shown in Eq. (2) [25]. However, to increase the accuracy of the empirical equation of the UEL for OX, Eq. (11) will be calculated from 150, 200 and 230 °C as initial temperatures to decide the UEL for OX. The prediction of UEL by the empirical model of Eq. (11) is practically close to the real UEL for OX. Finally, the coefficients d and e can be substituted to Eq. (11), as shown in Table 3.

As shown in Table 3, when initial pressure is increased, the coefficient d is decreased, but opposite for the coefficient e. These coefficients will be taken into Eq. (11) to forecast the UEL for OX under higher initial temperatures.

Table 3
Empirical UEL equation coefficients for OX under different pressures

Pressure (mmHg)	d	e
760	0.20	−0.037
1,520	0.17	−0.032
2,280	0.15	−0.027

Table 4
Empirical equation coefficients for OX under different temperatures

Temperature (°C)	a	b
100	0.03	0
150	0.18	0
200	0.17	0
230	0.16	0

$$\mathrm{UEL}\,(T_1) = \mathrm{UEL}\,(T_0) \times \left[1 + d\left(\frac{T_1 - T_0}{100}\right) + e\left(\frac{T_1 - T_0}{100}\right)\right] \quad (11)$$

If initial pressure is increased, then the UEL will be increased from literature. Therefore, the experimental data could be taken into Eq. (4) to calculate the coefficients a and b which can then be substituted to Eq. (12), as shown in Table 4.

As shown in Table 3, while initial temperature is increased, the coefficients a are decreased, along with all zeroes of the coefficients b. These coefficients could, in turn, be fed to Eq. (12) to predict the UEL for OX under higher initial pressures.

$$\mathrm{UEL}(P_1) = \mathrm{UEL}(P_0)\left[1 + f\left(\frac{P_1}{P_0} - 1\right)\right] \quad (12)$$

Commercially, the oxidation process could benefit from increasing the OX concentration as long as process conditions are well controlled with safe approaches. Therefore, based upon the experimental conditions, the oxygen concentration will be increased to 30 and 40 vol.% as oxygen concentration that can be, then, taken into the coefficients in Eq. (5) to estimate the UEL for OX under higher initial temperatures. As shown in Table 5, while keeping the initial temperature at 150 °C and increasing the initial pressure, the coefficient p is about a constant of 50 and the coefficient q is decreased to be a negative value, corresponding to the oxygen concentration ranging from 21 to 100 vol.%.

Therefore, the UEL for OX of empirical model under higher oxygen concentration is applied to estimate flammability zones completely and is provided

Table 5
Empirical equation coefficients for OX under different temperatures and pressures

Temperature (°C)	Pressure (mmHg)	p	q
100	760	45	−0.53
150	760	50	−0.55
150	1,520	50	−0.58

to the PA plant for proactive prevention of fire and explosion hazards.

In accord with the experimental results, the UEL under the process conditions of normal PA plants is in the range of 7.5 ± 0.25 to 7.75 ± 0.25 vol.%, respectively, which is within the flammable zone of OX in air. Potential fires or explosions may occur if there are ignition sources such as a flame or electrical spark, with enough energy.

6. Conclusions

6.1. Above normal boiling point of OX (>144 °C)

Under the experimental conditions, where OX are controlled by the same oxygen concentration, we have reached the following conclusions:

(I) If the initial temperature and initial pressure are increased, then the UEL and flammability zones of OX are correspondingly increased.
(II) In the meantime, if the initial temperature is increased, then the LEL of OX is decreased. But if the initial pressure is increased, the LEL is almost invariable.
(III) However, if the initial temperature is increased, then the P_{max} and K_g are conversely decreased. Whereas, if the initial pressure is increased, then the P_{max} and K_g are increased also.
(IV) Finally, if the initial temperature is increased, then the MOC is almost invariable. However, the MOC is decreased, while the initial pressure for OX is less than its normal boiling point.

6.2. Below normal boiling point of OX (<144°C)

As far as the liquid–vapour two-phase condition is concerned, the conclusions can be drawn as follows:

(I) If the initial temperature is set at 100 °C, while increasing the initial pressure, then the UEL and flammability zones of OX are correspondingly increased. Whereas the LEL variation is too small to be noticeable.
(II) Meanwhile, if the initial temperature is set at 100 °C and the initial pressure is increased, then the P_{max} and K_g are increased, too.
(III) If the initial temperature is set at 100 °C and the initial pressure is increased, then the MOC is conversely decreased. However, the MOC variation is not remarkable.

6.3. To combine all the above results, conclusions are drawn as follows

(I) The experimental results of OX showed that the UEL, P_{max} and K_g of OX are higher, under 100, than 150 °C, or even higher temperatures. Consequently, the liquid–vapour co-existing phase demonstrated a higher degree of hazard, in terms of the related explosion characteristic parameters.
(II) Specifically, MOC plays a crucially important role in this PA oxidation process. Here, the MOC of OX is decided by initial pressure, instead of initial temperature.
(III) In practice, process conditions for the normal PA plant are controlled under 370–410 °C as initial temperature and 760 mmHg as initial pressure. According to experimental results, the UEL under the process conditions of PA plant are 7.5 ± 0.25 to 7.75 ± 0.25 vol.%, respectively.
(IV) Based upon the experimental results, empirical flammability models can be established and, in turn, be used for calculation of flammability zones.
(V) In general, the plant operating conditions are well dictated to produce OX vapour compositions well above the UEL and hence the working atmosphere is nonflammable during the reaction period.
(VI) According to NFPA 69, the combustible concentration should be kept below 25% of the LEL [16].
(VII) From the experimental results, it is imperative that the loading of the volume concentration of OX should be adequately controlled not to fall

into its flammability zone under specific operating conditions.

7. Recommendations

(a) Establish the total solution for the PA plant by using a 20-L-Apparatus to test dust explosions and preventative measures for maleic anhydride (MA) and PA. [20,21].
(b) Study factors for PA production by OX on catalytic effects by using various instruments, such as GC–MS, for specific need.
(c) Conduct experiments on OX at various initial temperatures such as 50, 75 °C to investigate its behaviours under liquid–vapour co-existing phase.
(d) Replace N_2 by different inert gases, such as CO_2 or H_2O, to differentiate individual effects on the flammability behaviours and related explosion characteristic parameters for OX tests.
(e) Compare the results of OX with 20-L-Apparatus and the 1-L-Apparatus, as shown in Fig. 16.
(f) Establish explosion characteristic parameters for OX, MX, PX and ethylbenzene (EB), so that a wide spectrum of C_8H_{10} series flammability models and flammability zones can be accomplished for each flammability model and flammability zone.

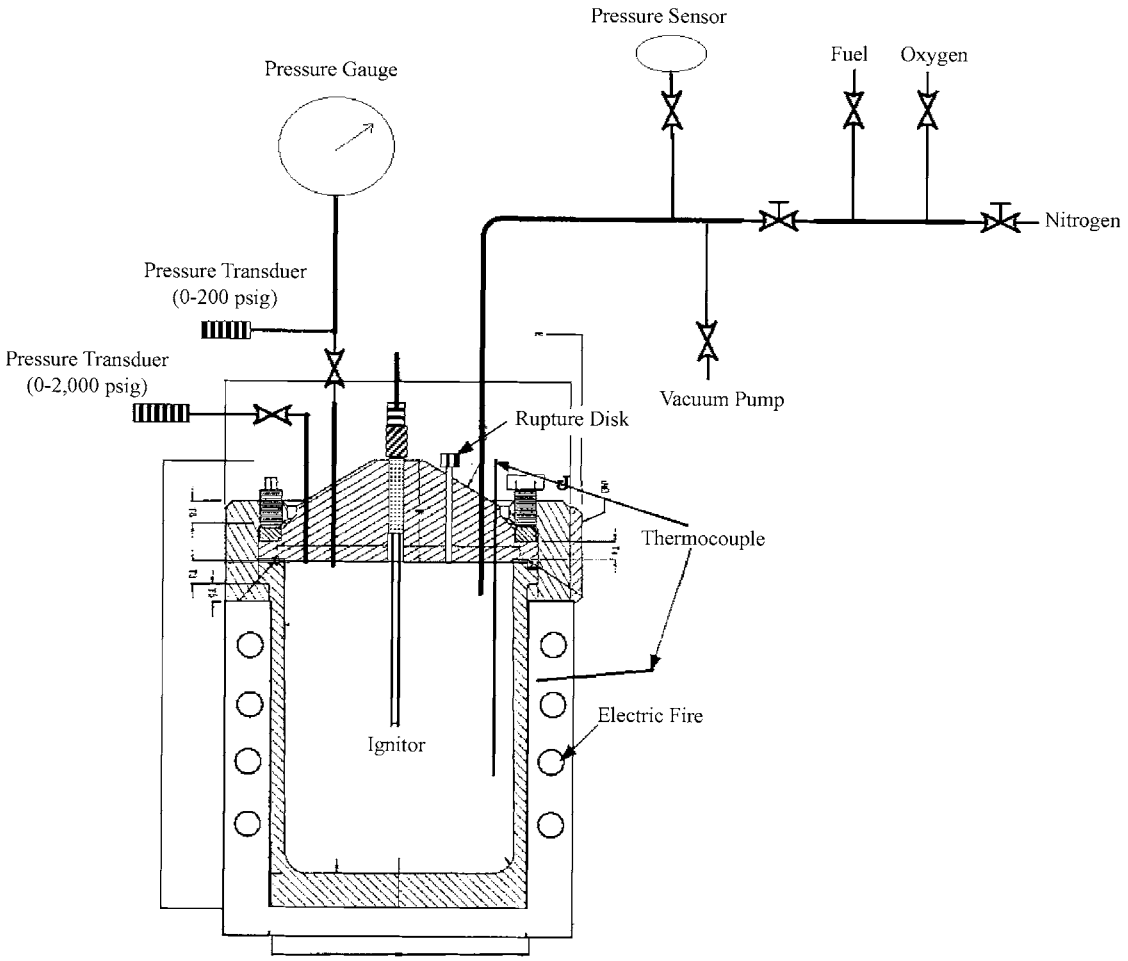

Fig. 16. A schematic diagram of 1-L-Apparatus for the determination of explosion characteristics of OX.

Acknowledgements

The authors wish to thank Dr. S.C. Huang at National Chiao Tung University and the Ministry of Education of ROC for financial support through the program of the Education Improvement for Civil Disaster Prevention. Finally, special appreciation goes to Mr. Chun-Fu Liang, PA Plant Manager of Nan Ya Plastics Corporation, for generously providing information and a supply of OX sample.

References

[1] ASTM, American Society for Testing and Materials, Standard Test Method for Concentration Limits of Flammability of Chemicals, Philadelphia, PA, USA, 1991, pp. E681–685.
[2] ASTM, American Society for Testing and Materials, Standard Practice for Determining Limits of Flammability of Chemicals at Elevated Temperature and Pressure, Philadelphia, PA, USA, 1993, pp. E981–983.
[3] W.E. Baker, et al., Explosion Hazards and Evaluation, Elsevier, New York, USA, 1992.
[4] M. Caron, et al., J. Hazard. Mater. A65 (1999) 233–244.
[5] V.M. Chad, A.C. Daniel, Process Safety Progr. 17 (3) (1998) 176–183.
[6] Chem. Systems Inc., Menlo Park, California, USA, 1995, pp. 10–17.
[7] D.A. Crowl, J.F. Louvar, Chemical Process Safety: Fundamentals with Applications, NJ, USA, 1990, pp. 157–192.
[8] H.F. Coward, G.W. Jones, Bureau of Mines Bulletion, 1952, p. 503.
[9] J.J. Graham, P.F. Way, Chem. Eng. Progr. 66 (1962) 54–58.
[10] J.J. Graham, Chem. Eng. Progr. 66 (9) (1970) 54–58.
[11] G.W. Jones, Chem. Rev. 22 (1) (1938) 1–26.
[12] W. Jost, Explosion and Combustion Process in Gases, McGraw-Hill, New York, USA, 1955, p. 56.
[13] F.P. Lees, Loss Prevention in the Process Industries, 2nd Edition, Vol. 2, Butterworth/Heinemann, London, 1996, pp. 140–172.
[14] R.J. Lewis, SAX'S Dangerous Properties of Industrial Materials, 9th Edition, Vol. 4, Nostrand Reinhold (Van), New York, 1996, p. 3404.
[15] NFPA 68, National Fire Protection Association, Guide for Venting of Deflagrations, Quincy, MA, USA, 1999.
[16] NFPA 69, National Fire Protection Association, Standard on Explosion Prevention System, Quincy, MA, USA, 1999.
[17] Operating Instructions for the 20-L-Apparatus. Kühner, Birsfelden, Switzerland, 1996, pp. 6–66.
[18] D. O'Shaughnessey, B. Power, Process Safety Progr. 14 (1) (1995) 22–25.
[19] C.M. Park, R.J. Sheehan, Phthalocyanine Compounds, in: Kirk-Othmer (Ed.), Encyclopedia of Chemical Technology, 4th Edition, Vol. 18, New York, USA, 1996, pp. 991–1043.
[20] R.F. Schwab, Dust Explosion, in: J.J. McKetta, W.A. Cunningham (Eds.), Encyclopedia of Chemical Processing and Design, Vol. 17, New York, USA, 1991, pp. 67–96.
[21] R.F. Schwab, W.H. Doyle, Chem. Eng. Progr. 66 (9) (19707) 49–53.
[22] R. Siwek, J. Loss Prev. Process Ind. 9 (1) (1996) 21–31.
[23] C.M. Shu, et al., in: Proceedings of the Conference on North American Thermal Analysis Symposium, Ottawa, Canada, 2000.
[24] C.M. Shu et al., in: Proceedings of the 17th Annual Conference on Asia Pacific Occupational Safety and Health Organisation, Taipei, Taiwan, 2001, pp. 443–465.
[25] B. Vanderstraeten, et al., J. Hazard. Mater. 56 (1997) 237–246.
[26] M.G. Zabetakis, S. Lambiris, G.S. Scott, in: Proceedings of the Seventh Symposium on Combustion, 1959, p. 484.
[27] M.G. Zabetakis, in: Proceedings of the Symposium of AIChE Institute of Chemical Engineering on Chemical Engineering Extreme, Conduction, Sec. 2, 1965, pp. 99–104.